Supporting Information

Engineering Li^+-selective quasi-solid electrolytes via zwitterion and poly(ethylene glycol) co-grafting on poly(arylene ether sulfone) for high-performance lithium–sulfur batteries

*Anh Le Mong, Jong Chan Shin, Minjae Lee, and Dukjoon Kim**

A. L. Mong, Prof. D. Kim
School of Chemical Engineering, Sungkyunkwan University, Suwon, Gyeonggi-do, 16419, Republic of Korea.
E-mail: djkim@skku.edu

Dr. J. C. Shin, Prof. M. Lee
Department of Energy Science & Engineering, Department of Chemistry, Kunsan National University, Gunsan, Jeollabuk-do, 54150 Republic of Korea.
E-mail: minjae@kunsan.ac.kr.

Number of page: 28

Number of figure: 20

Experimental procedure

Preparation of ionic liquid (IL) A solution containing 1-iodobutane (9.5 g, 0.05 mol) in THF (5 mL) was gradually introduced dropwise into a solution of N-methylpyrrolidine (5 g, 0.05 mol) dissolved in ethyl acetate (15 mL). The reaction system was maintained under stirring at 45 °C for 8 h. The precipitated solid was separated by filtration and subsequently washed three times with ethyl acetate. The obtained material was dried in a vacuum oven at ambient temperature for 30 h, yielding PYR–I. PYR–I (4.8 g) was then combined with $LiTf_2N$ (5 g) in deionized water (4.5 g), and the mixture was stirred until phase separation occurred after 8 h. The denser phase was isolated, filtered, and rinsed with cold water to eliminate residual salts. Finally, the product was subjected to freeze-drying for 48 h, affording pure PYR–Tf_2N ionic liquid (3.0 g, 75% yield).

Synthesis of poly(arylene ether sulfone) (PAES) Diphenolic acid (8.58 g, 0.03 mol) and bis(4-fluorophenyl) sulfone (7.62 g, 0.03 mol) were introduced into a 500 mL three-neck round-bottom flask containing dimethyl sulfoxide (75 g) and toluene (68 g) at 165 °C. The reaction mixture was maintained under these conditions for 52 h, after which it was cooled to room temperature. The resulting solids were collected by filtration and subsequently dissolved in a mixture of tetrahydrofuran (45 mL) and hydrochloric acid (36.5 M, 10 mL) to yield a light yellow solution. The solution was then precipitated into 750 mL of isopropanol, affording white PAES solids. The solids were washed with deionized water and dried under vacuum at 85 °C, yielding PAES (14.2 g, 88%).

Results and Discussion

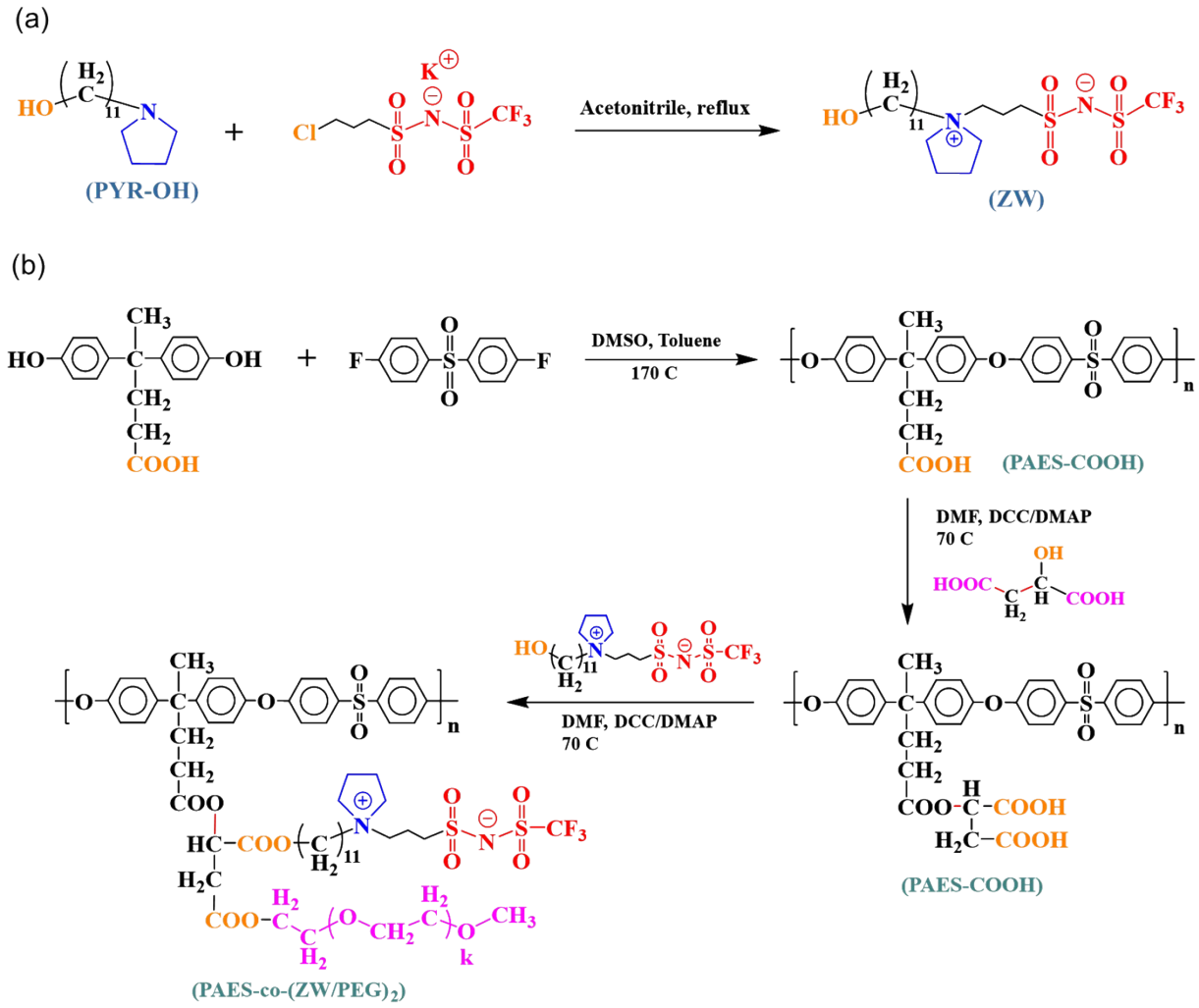

Figure S1. Synthetic scheme of (a) N-(((3-[1-(11-Hydroxyundecyl) pyrrolidinium)] propyl) sulfonyl) trifluoromethane-sulfonyl) imide zwitterion; and (b) PAES-*co*-(ZW/PEG)$_2$.

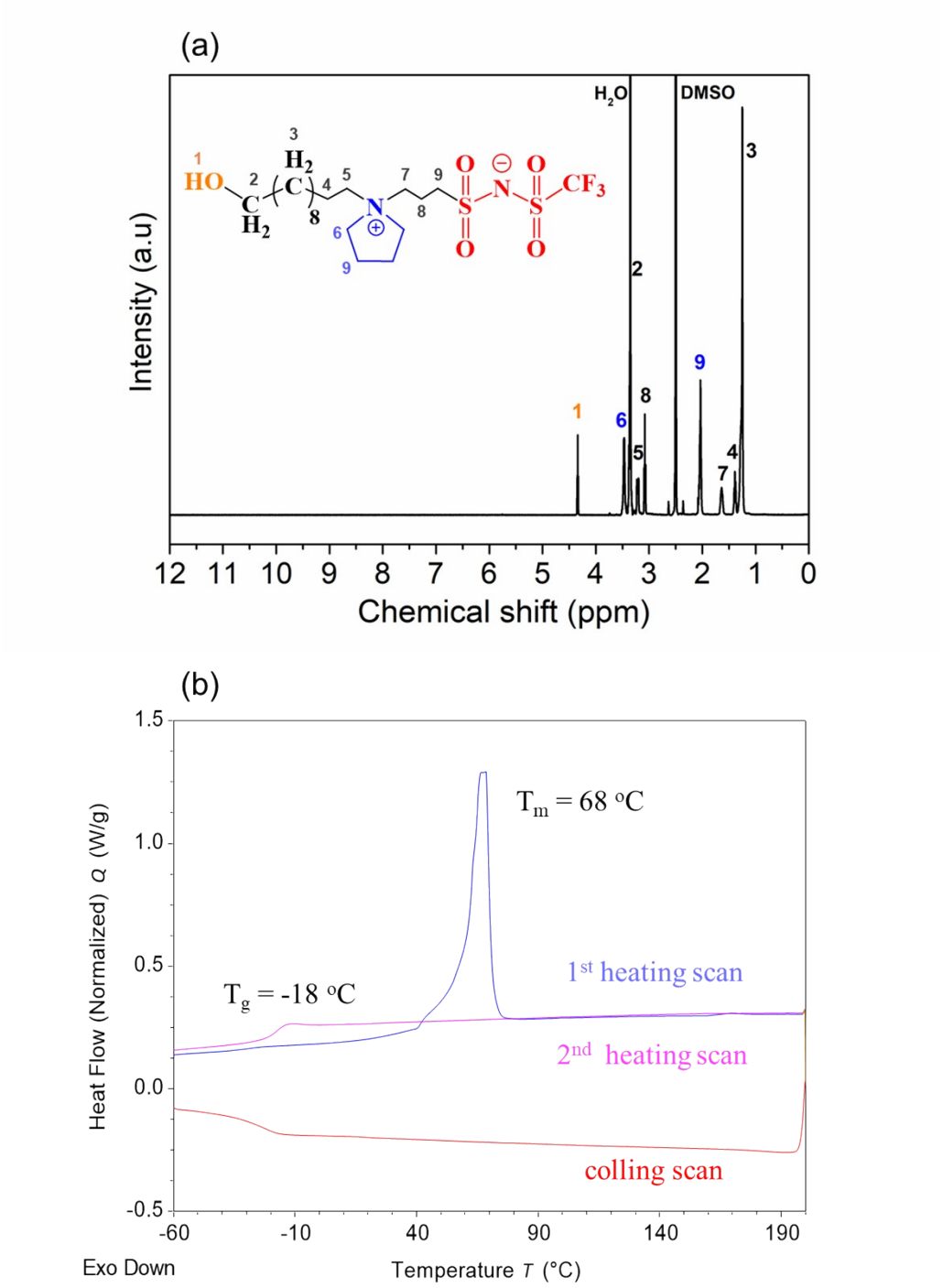

Figure S2. (a) NMR spectrum; and (b) DSC curves of zwitterion (ZW).

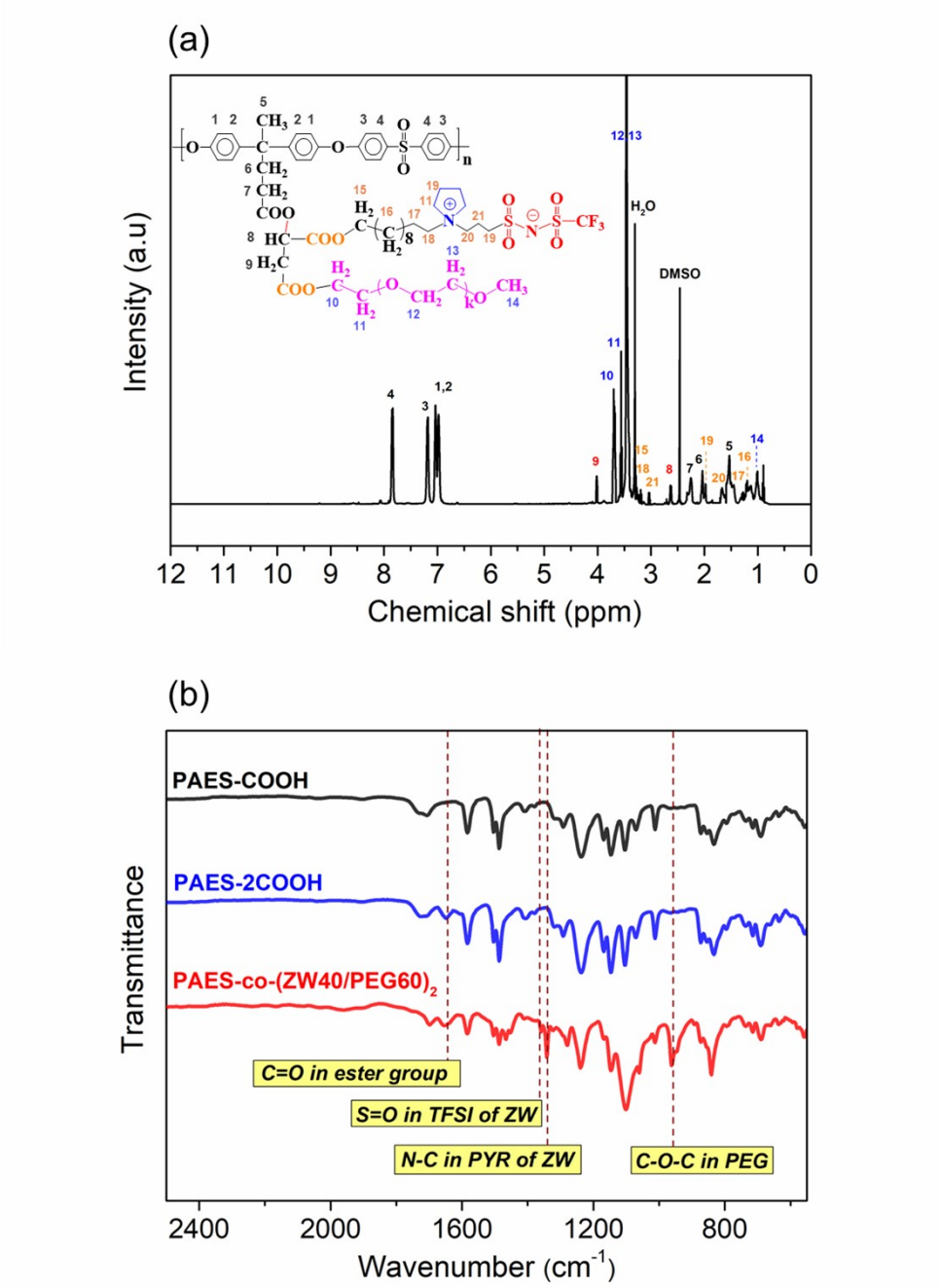

Figure S3. (a) NMR spectrum of PAES-co-(ZW/PEG)$_2$; and (b) FTIR spectra of PAES, PAES-2COOH and PAES-co-(ZW/PEG)$_2$.

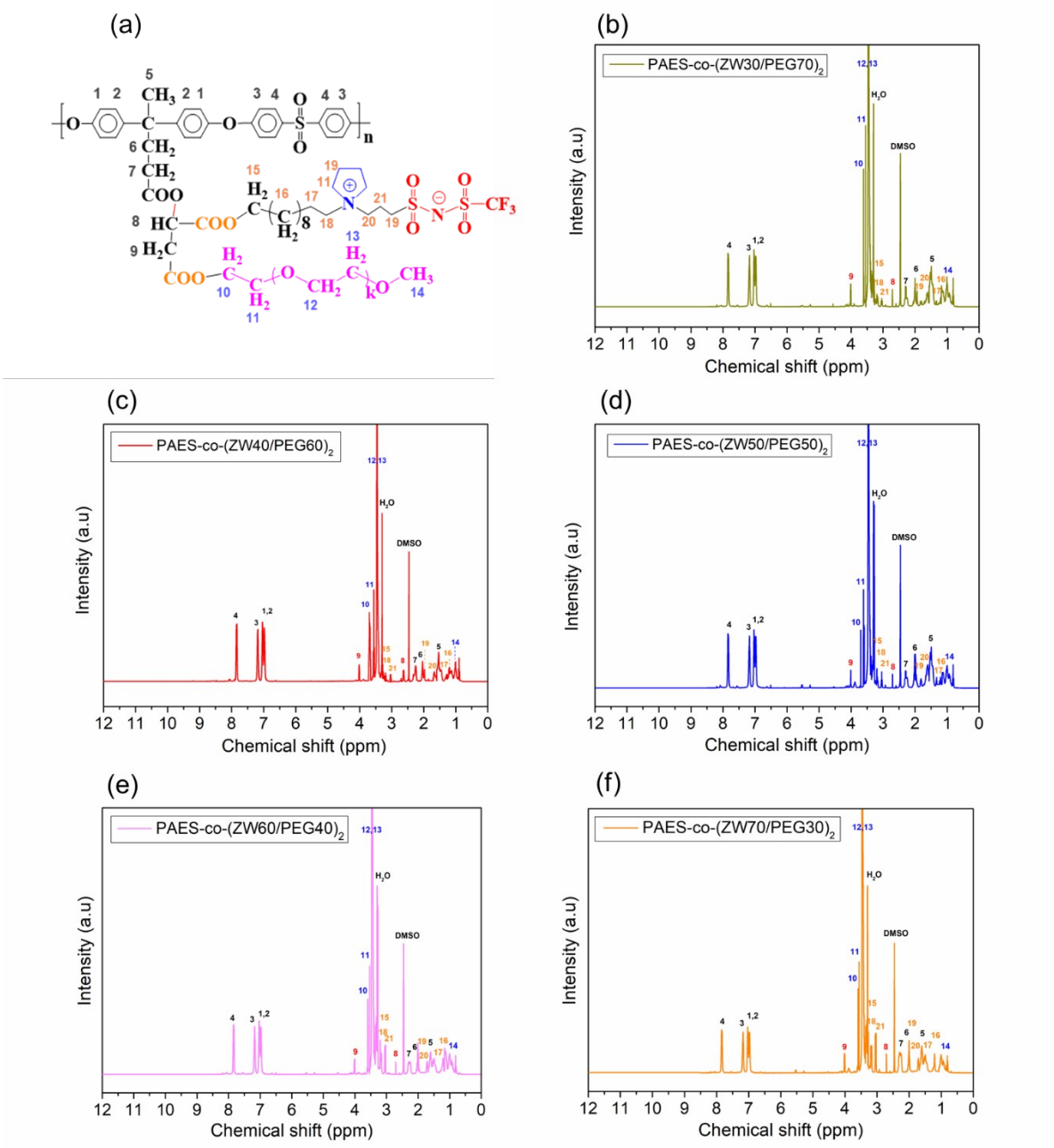

Figure S4. (a) Chemical structure of PAES-co-(ZW/PEG)$_2$; and (b-f) 1H-NMR spectra of PAES-co-(ZW/PEG)$_2$ with different ZW/PEG ratios.

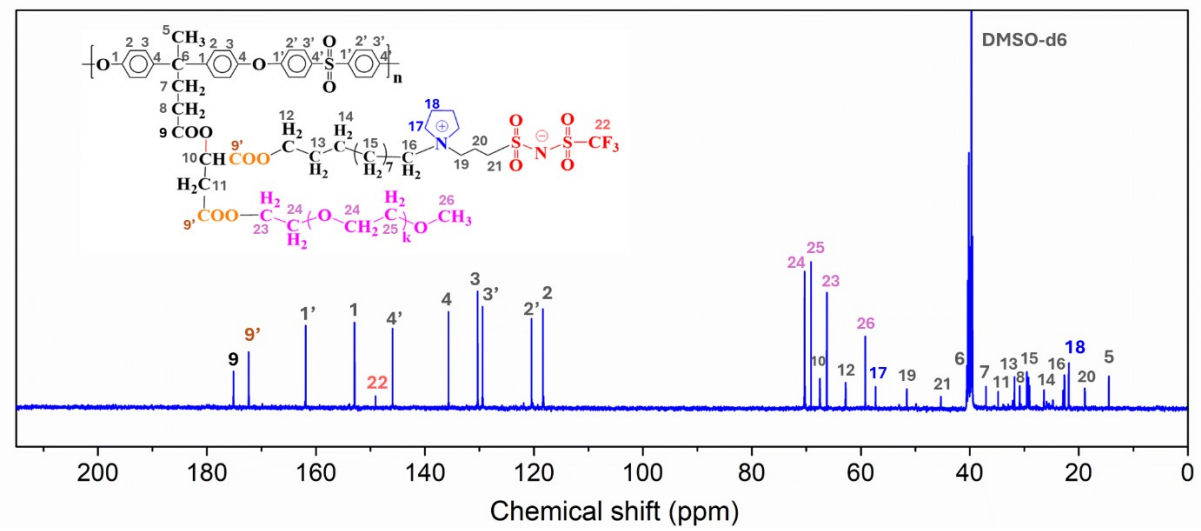

Figure S5. ^{13}C-NMR spectrum of PAES-co-(ZW40/PEG60)$_2$ membranes.

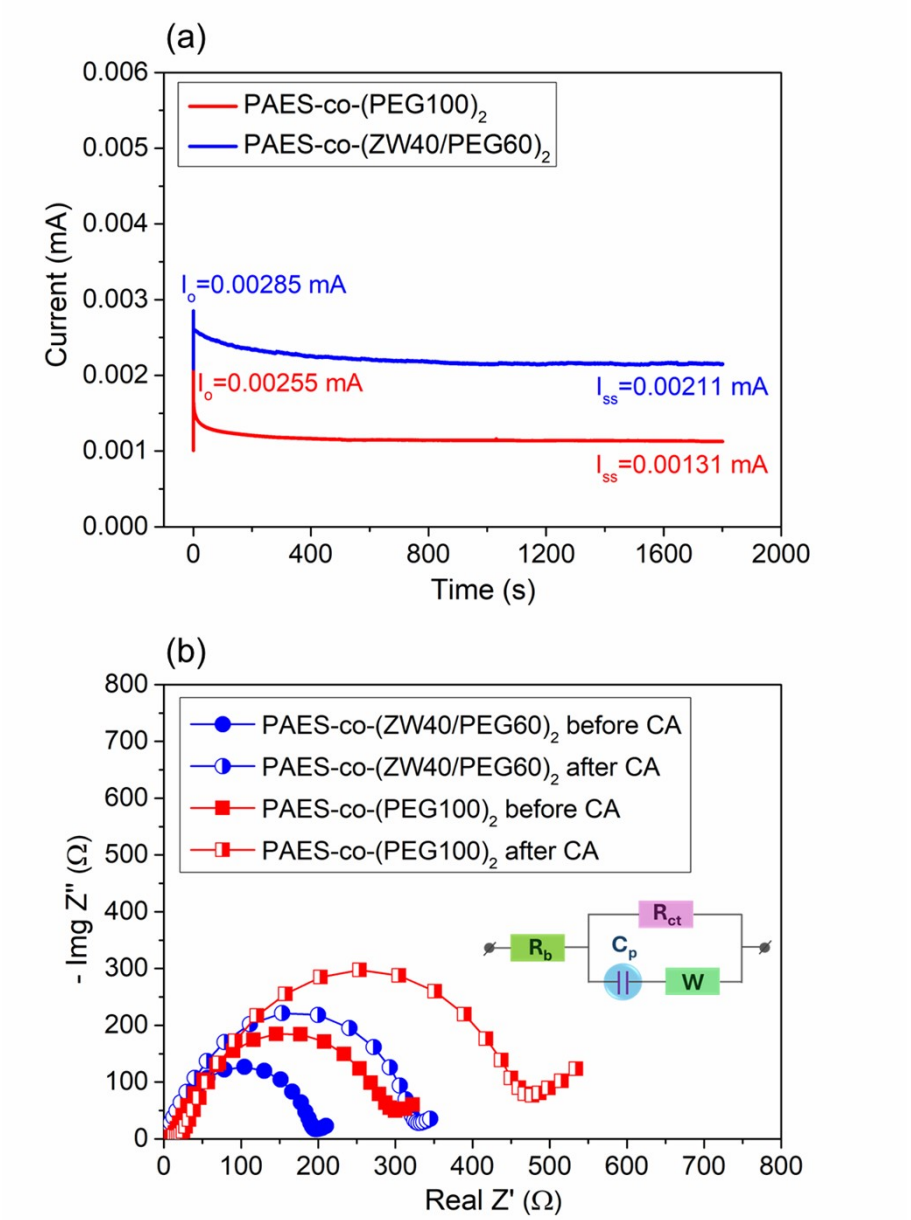

Figure S6. (a) CA profiles; and (b) impedance before and after CA test of PAES-co-$(PEG100)_2$ and PAES-co-$(ZW40/PEG60)_2$ membranes.

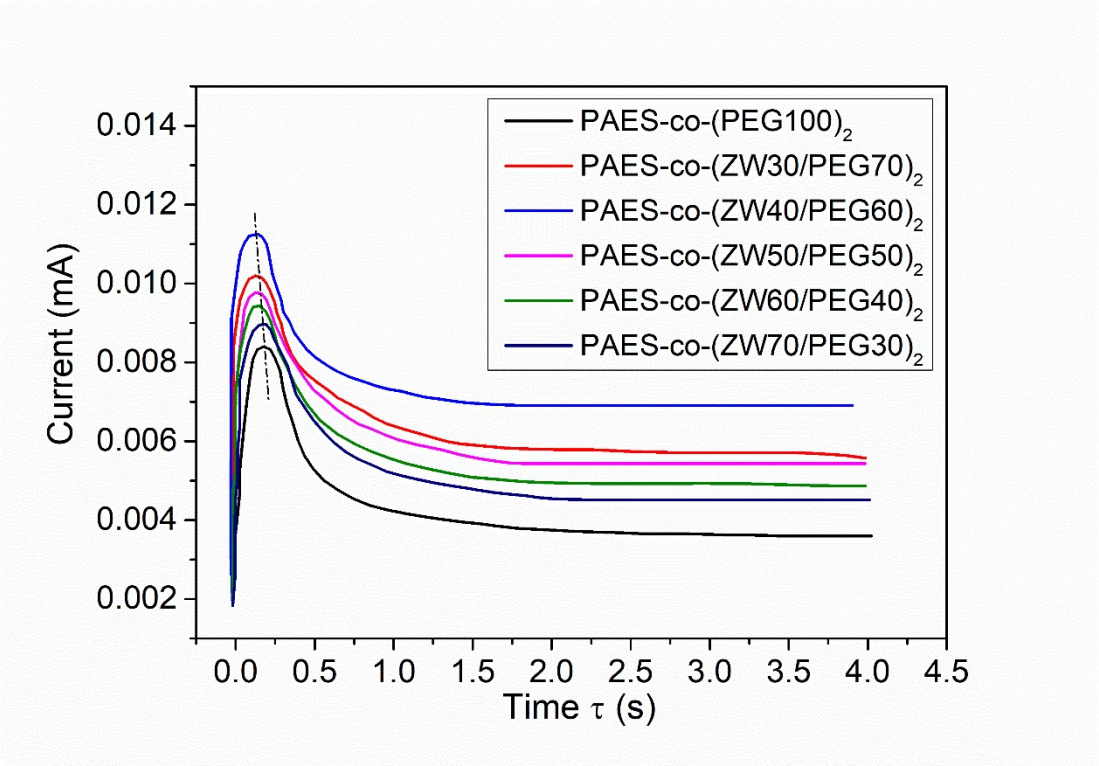

Figure S7. Transient ion current (TIC) curves of PAES-co-$(PEG100)_2$ and PAES-co-$(ZW/PEG)_2$ membranes at different ZW/PEG ratios.

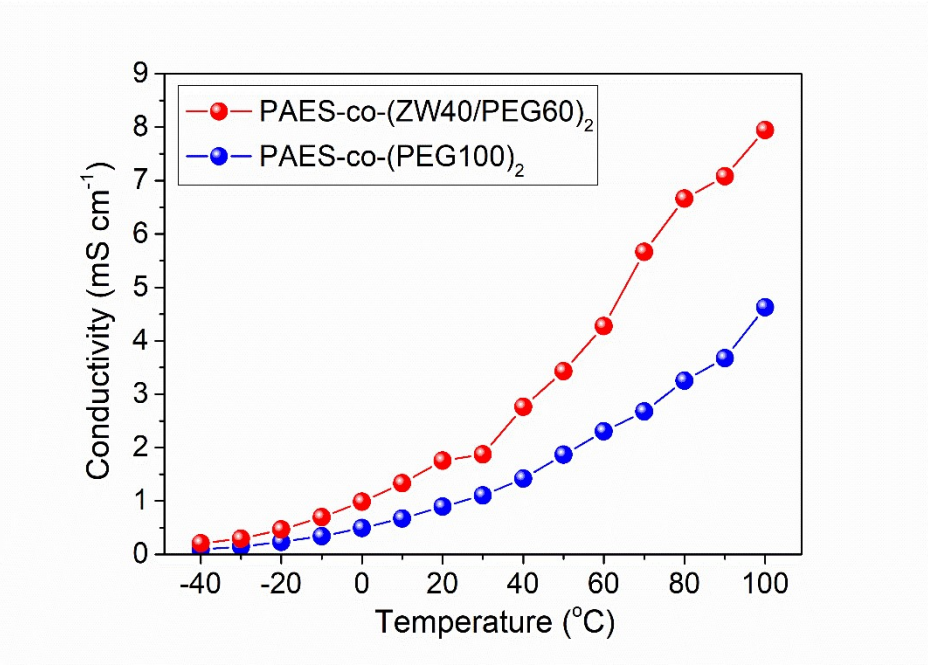

Figure S9. Thermal activation energy of PAES-co-$(PEG100)_2$ and PAES-co-$(ZW40/PEG60)_2$ membranes.

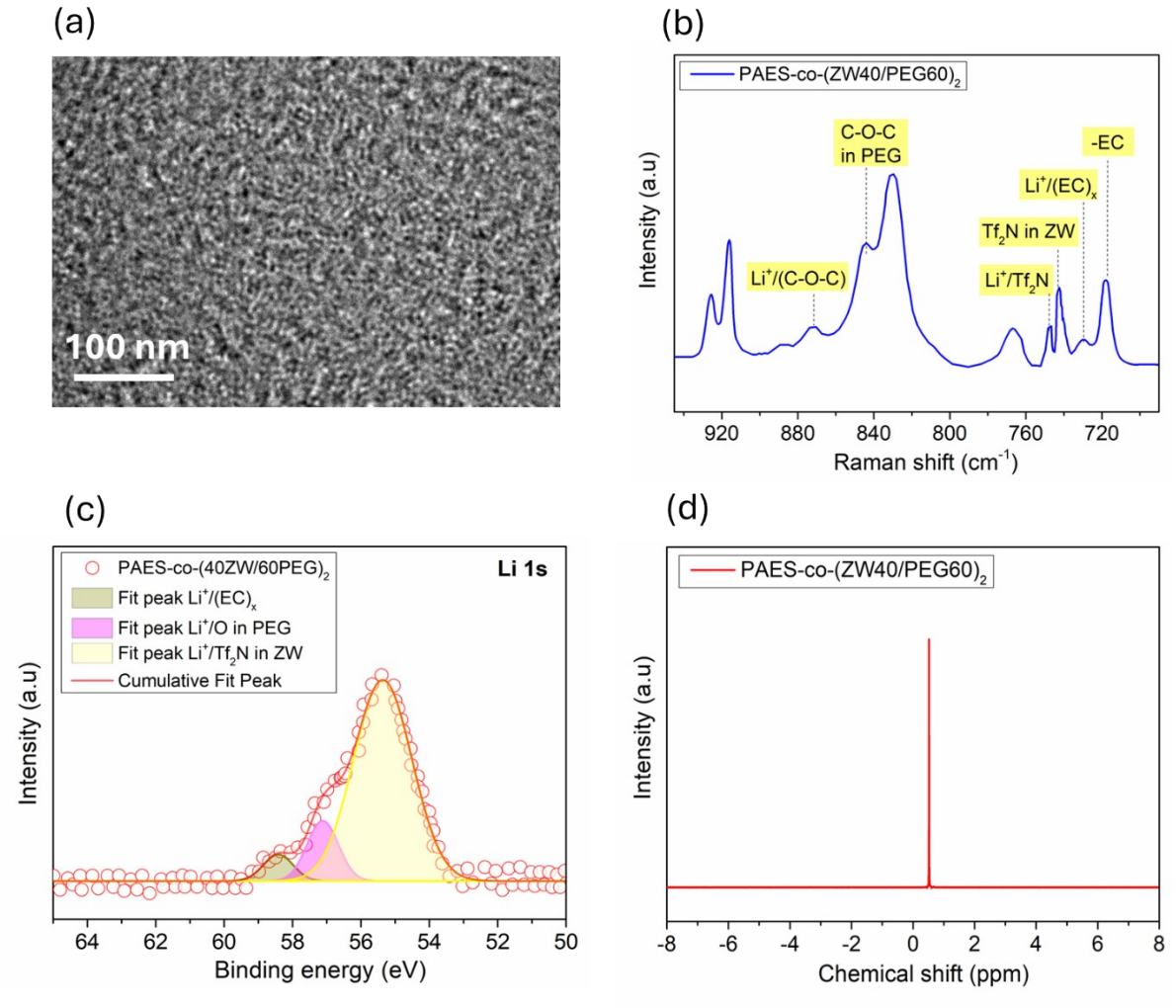

Figure S9. (a) TEM image; (b) Raman spectrum; (c) Li 1s XPS curve; and (d) Li-NMR spectrum of PAES-co-(ZW40/PEG60)$_2$ membranes.

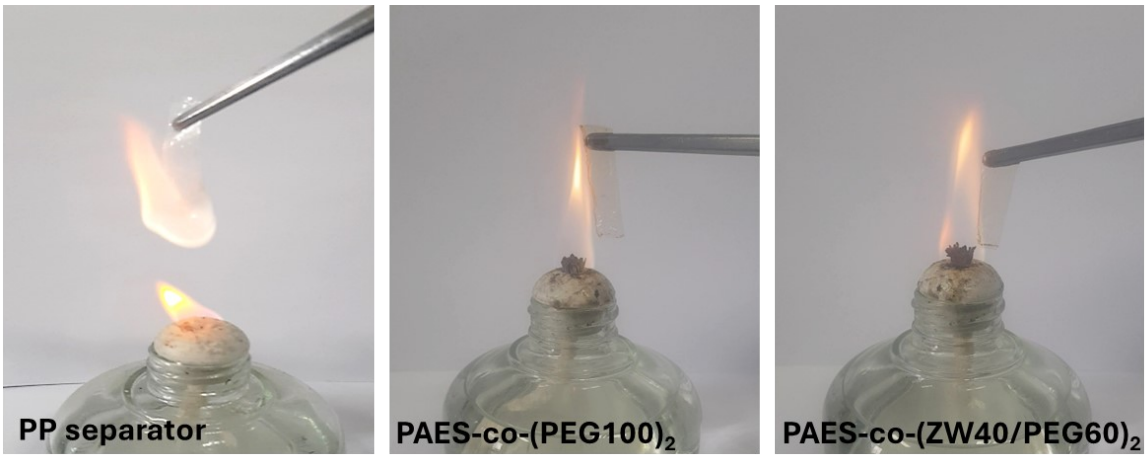

Figure S10. Flamamability test of PP separator; PAES-co-$(PEG100)_2$ and PAES-co-$(ZW40/PEG60)_2$ membranes containing 70 wt.% (IL-EC).

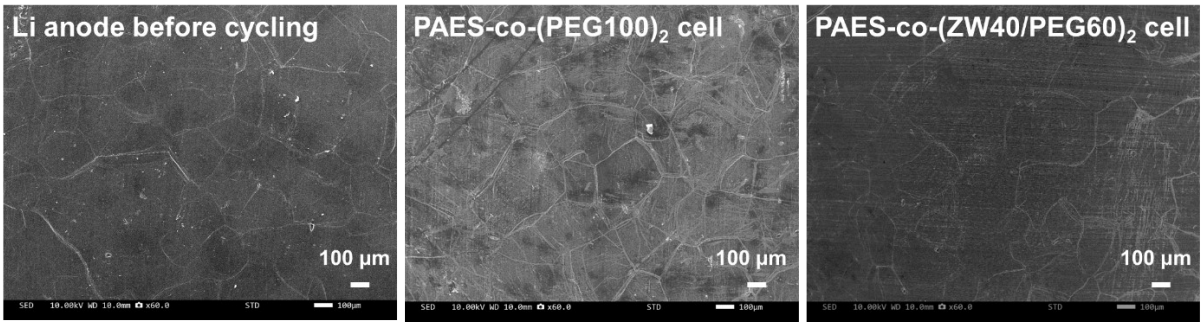

Figure S11. SEM images of Li-anode before before and after 1000 h cycling at 2.0 mA cm^{-1} for Li/SPE/Li cell assembled with PAES-co-$(PEG100)_2$ and PAES-co-$(ZW40/PEG60)_2$ membranes containing 70 wt.% (IL-EC).

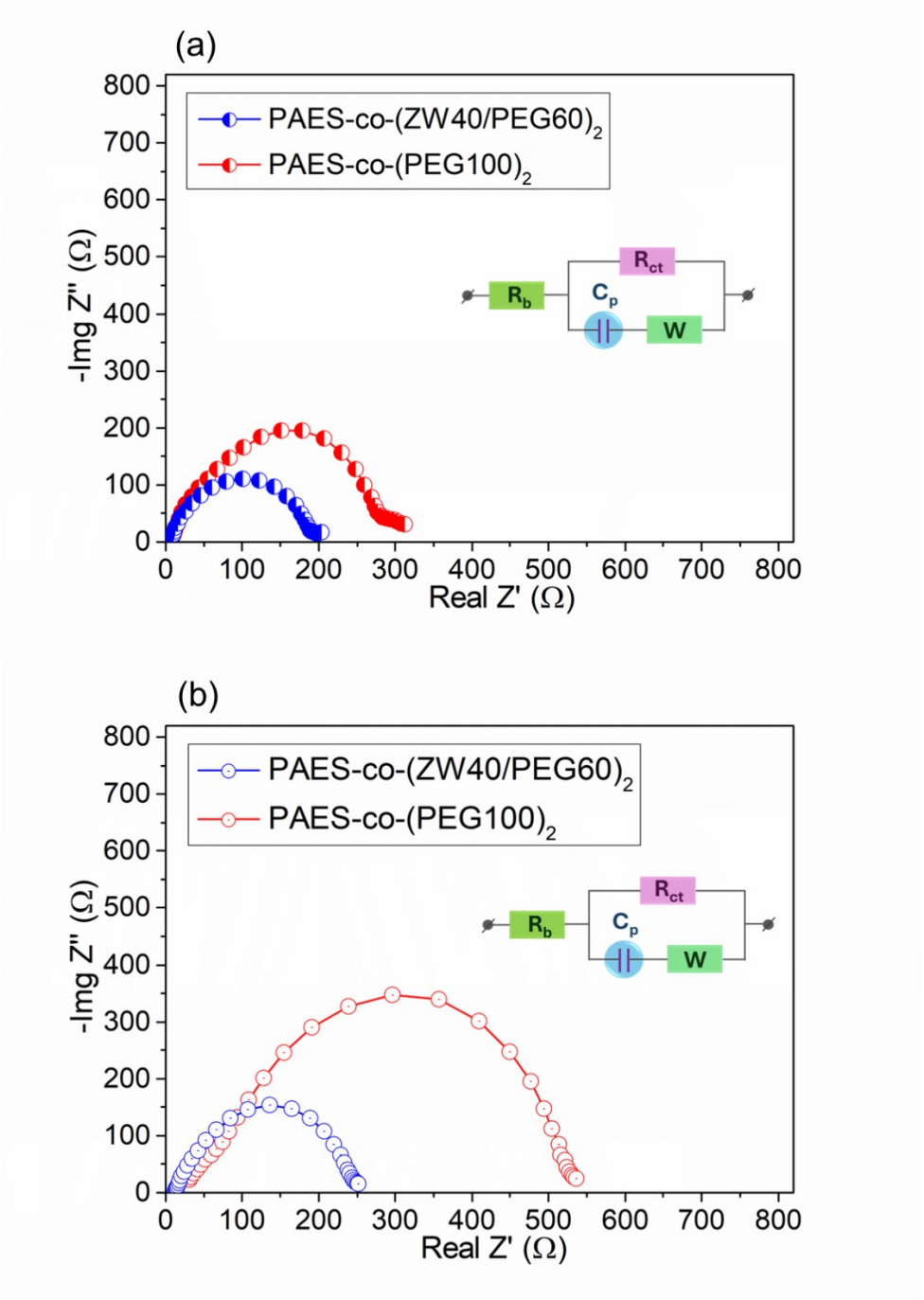

Figure S12. EIS plots (a) before and (b) after 1000 h cycling at 2.0 mA cm^{-1} for Li/SPE/Li cell assembled with PAES-co-$(PEG100)_2$ and PAES-co-$(ZW40/PEG60)_2$ membranes containing 70 wt.% (IL-EC).

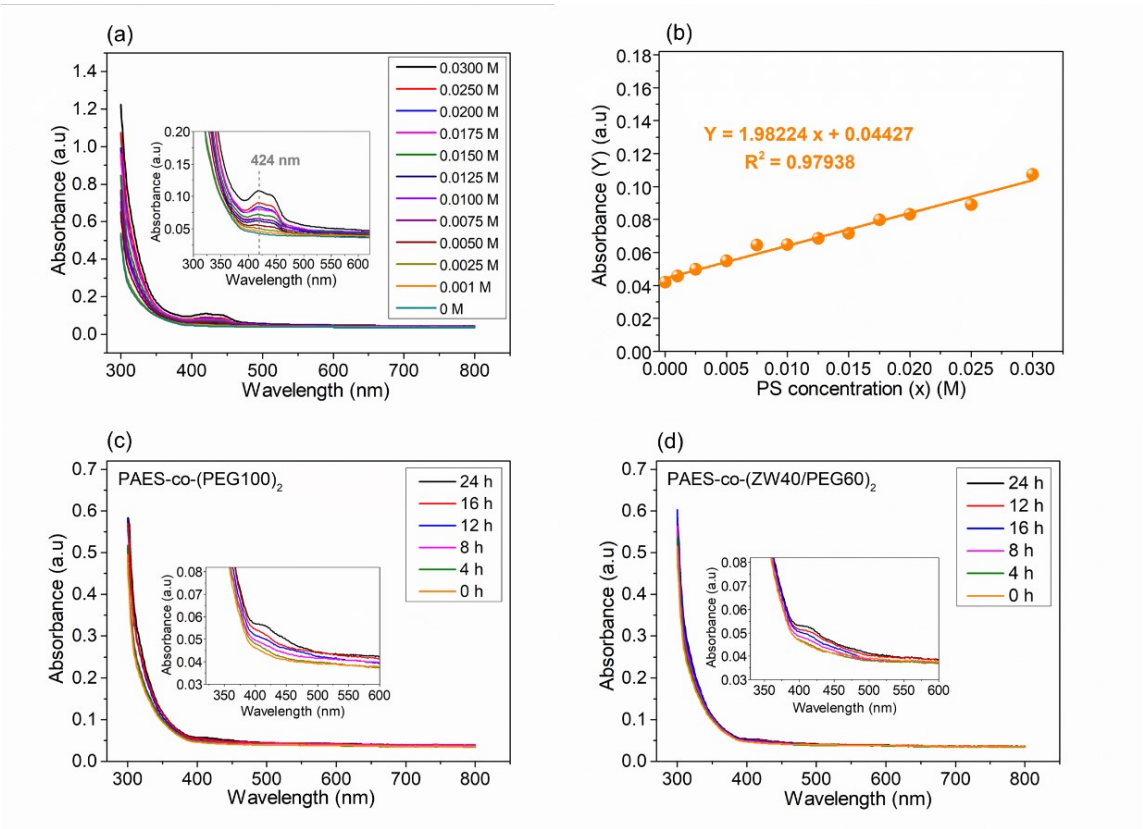

Figure S13. (a) UV-vis spectra of PS solution at different concentrations; (b) calibration plot of absorbance vs. PS concentration with the linear regression; (c-d) UV-vis spectra of PS solution diffused through PAES-co-$(PEG100)_2$ and PAES-co-$(ZW40/PEG60)_2$ membranes containing 70 wt.% (IL-EC).

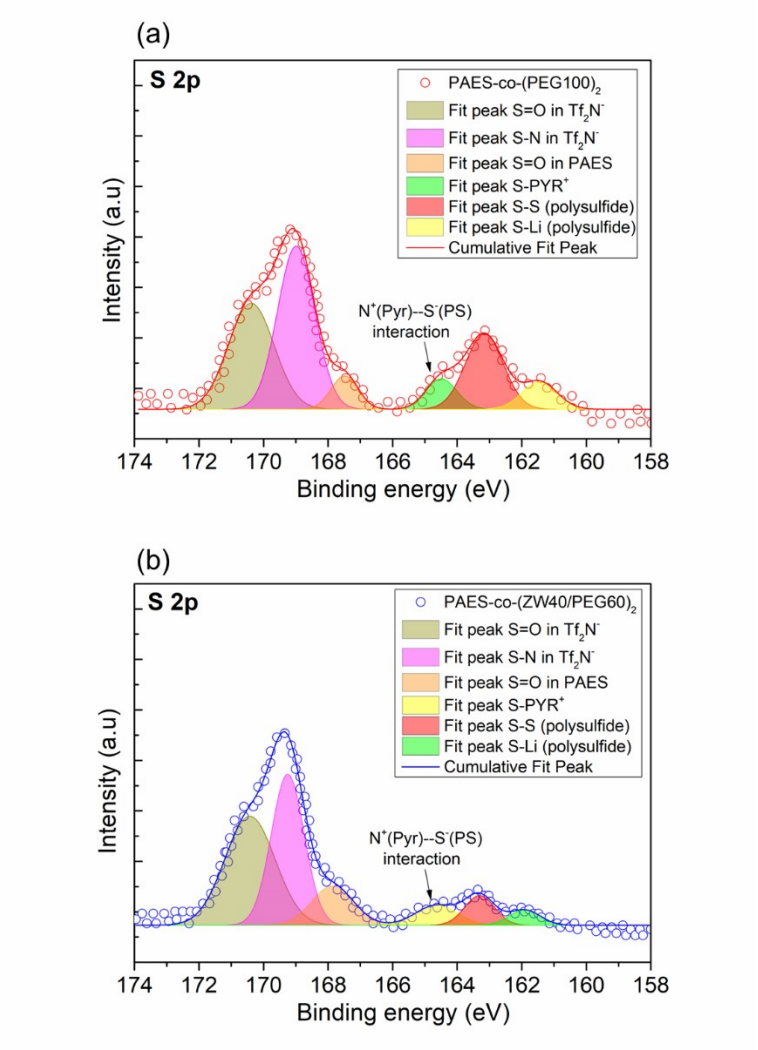

Figure S14. High resolution S2p XPS spectra of (a) PAES-co-$(PEG100)_2$; and (b) PAES-co-$(ZW40/PEG60)_2$ membranes after PS permeability test.

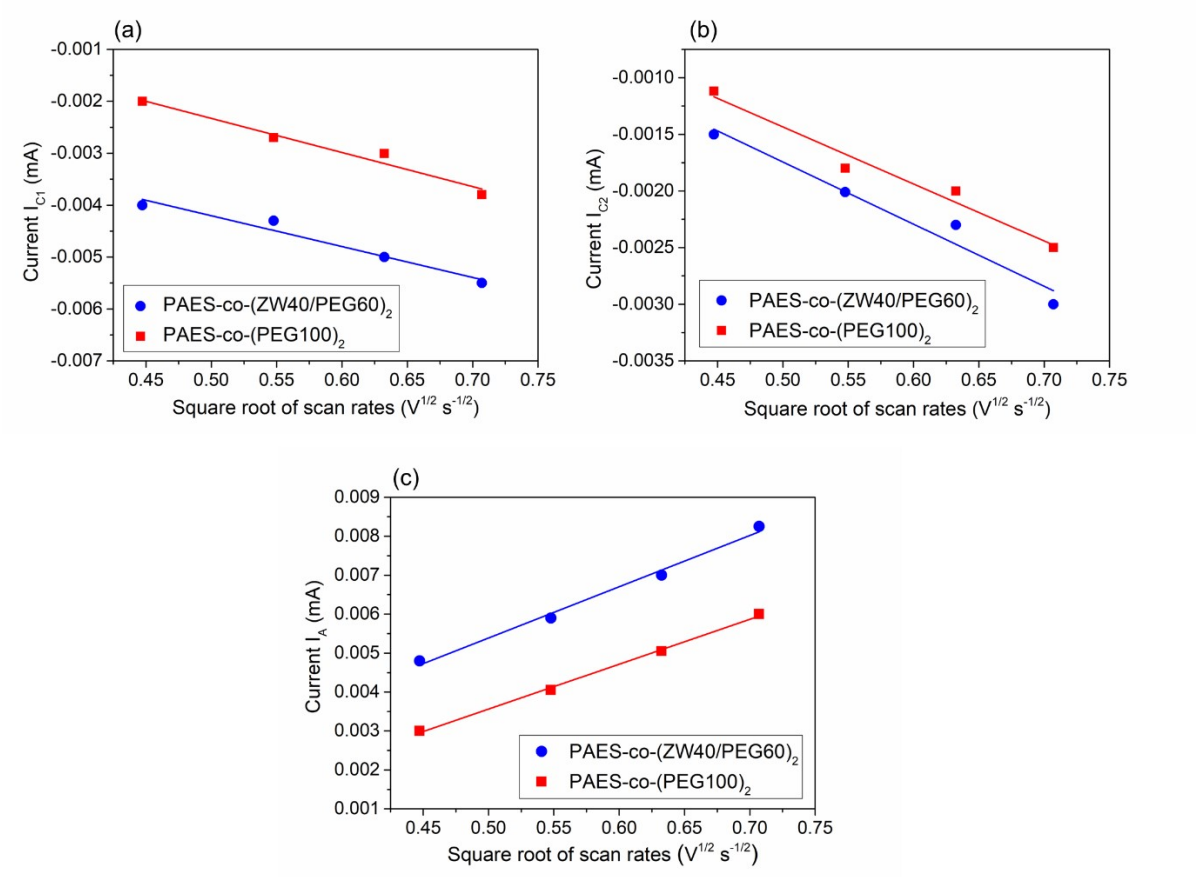

Figure S15. Fitting linear curves of current peak *(I) vs.* $v^{0.5}$ using the Randles–Sevcik model at (a) peak cathode 1; (b) peak cathode 2; and (c) peak anode.

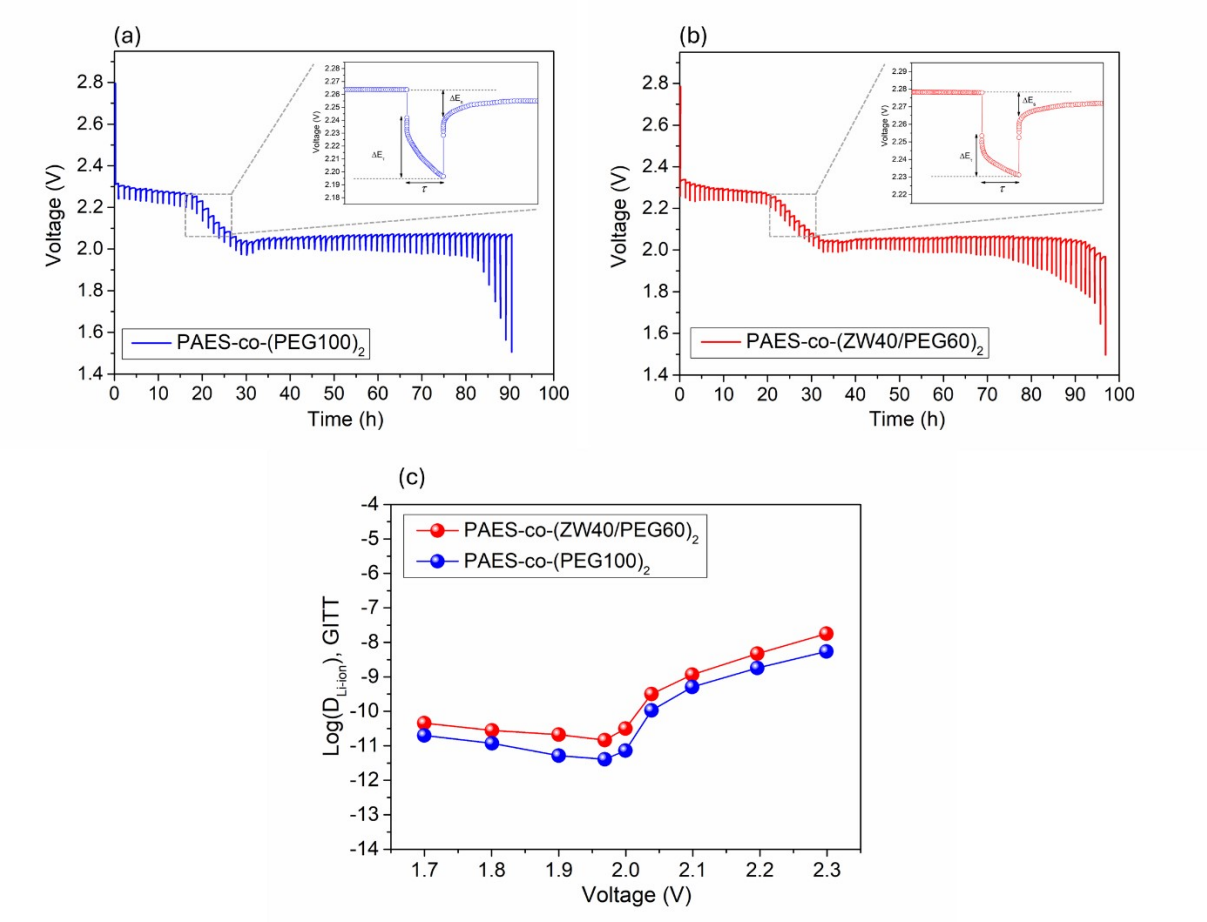

Figure S16. (a-b) GITT curves and (c) Li-ion diffusion ($D_{Li\text{-}ion}$)$^{(*)}$ in S/SPE/Li cells assembled with PAES-co-(PEG100)$_2$; and (b) PAES-co-(ZW40/PEG60)$_2$ membranes at 0.2 C in voltage range of 2.8 -1.5 V.

(*) $D_{Li\text{-}ion}$ were calculated from Weppner-Huggins equation as follows:

$$D_{Li-ion} = \frac{4}{\pi} \times \left(\frac{m_B \times V_M}{M_B \times S}\right)^2 \times \left(\frac{\Delta E_s}{\Delta E_\tau}\right)^2 \times \frac{1}{\tau}$$

Where, τ is duration of the current pulse (τ = 5 minutes); m_B is mass of active sulfur material (m_B = 5.0 mg); M_B is molar mass of sulfur; V_M is molar volume of sulfur electrode material (cm^3 mol^{-1}); S is effective electrode–electrolyte contact area (S= 1.1304 cm^2); ΔE_τ and ΔE_s are total voltage change during the current pulse (excluding IR drop) and the steady-state voltage change after relaxation, respectively.

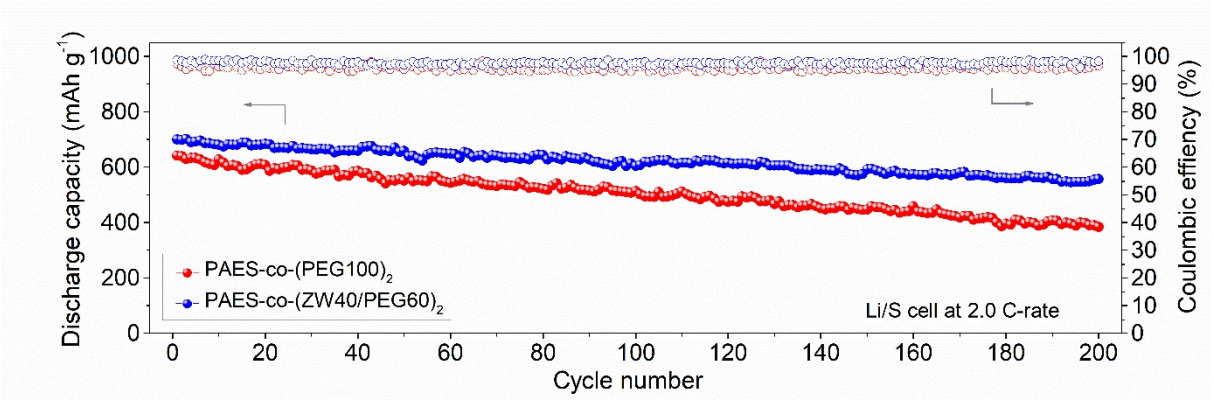

Figure S17. Cycling performance of Li/S cells assembled with PAES-co-$(PEG100)_2$ and/or PAES-co-$(ZW40/PEG60)_2$ membrane at 2.0 C-rate.

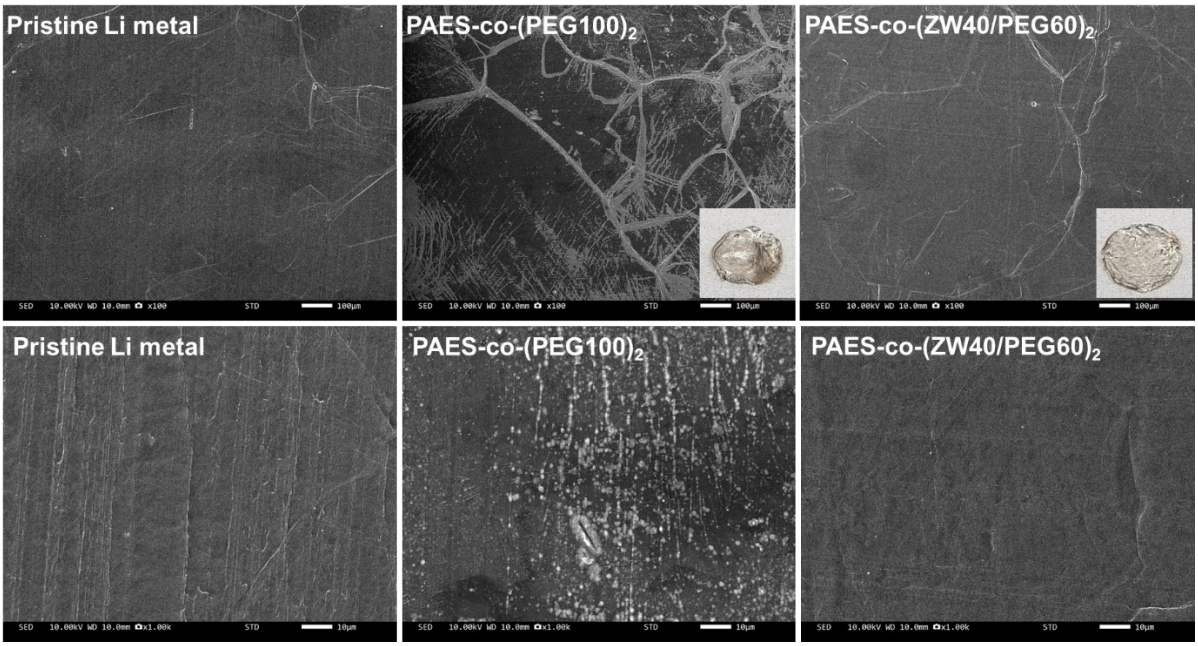

Figure S18. SEM images of Li-surface in S/SPE/Li cells assembled with PAES-co-$(PEG100)_2$; and (b) PAES-co-$(ZW40/PEG60)_2$ membranes after 300 cycles at 0.2 C in voltage range of 2.8 -1.5 V.

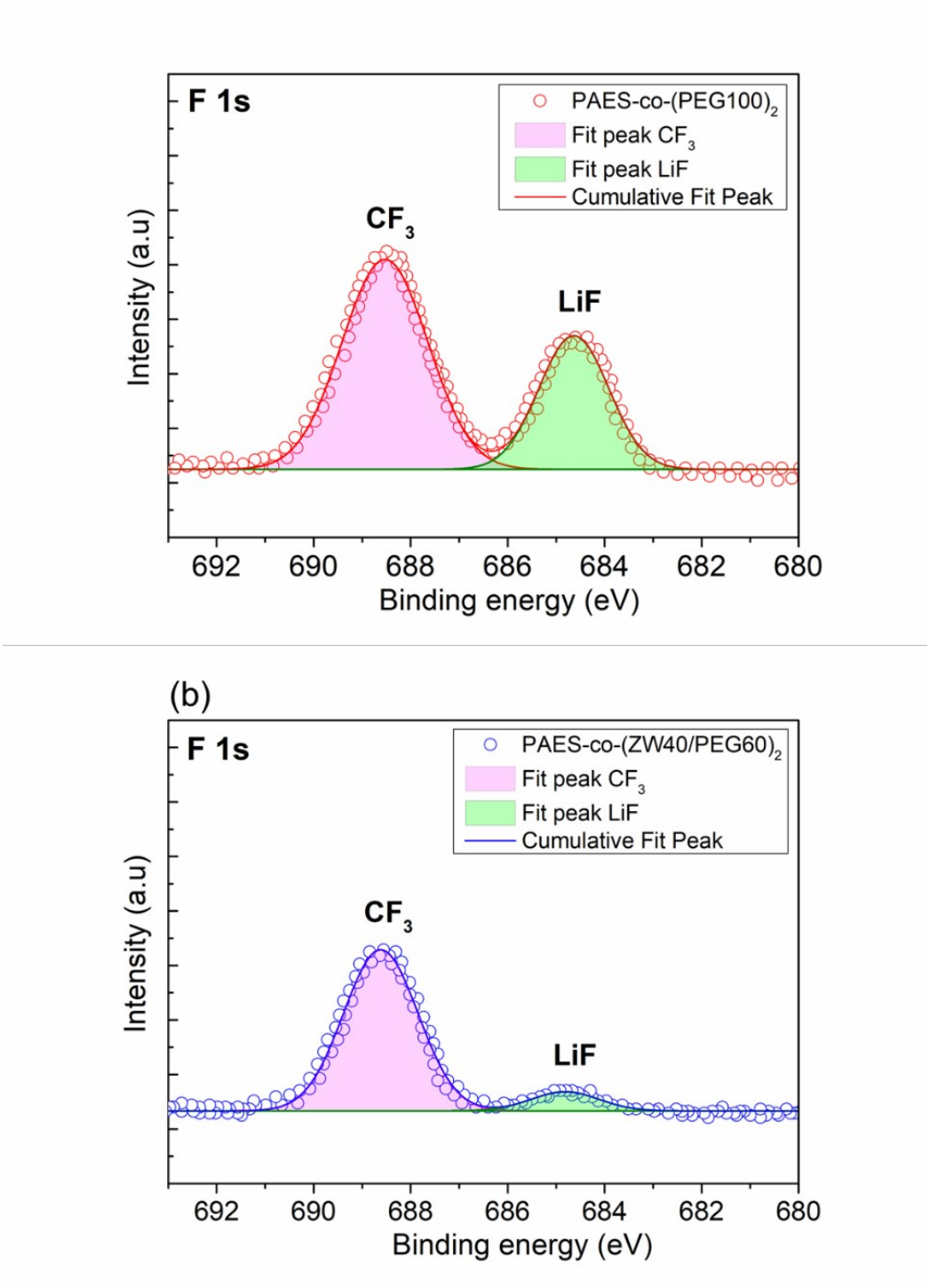

Figure S19. High resolution F1s XPS spectra of lithium surface in S/SPE/Li cells assembled with PAES-co-$(PEG100)_2$; and (b) PAES-co-$(ZW40/PEG60)_2$ membranes after 300 cycles at 0.2 C in voltage range of 2.8 -1.5 V.

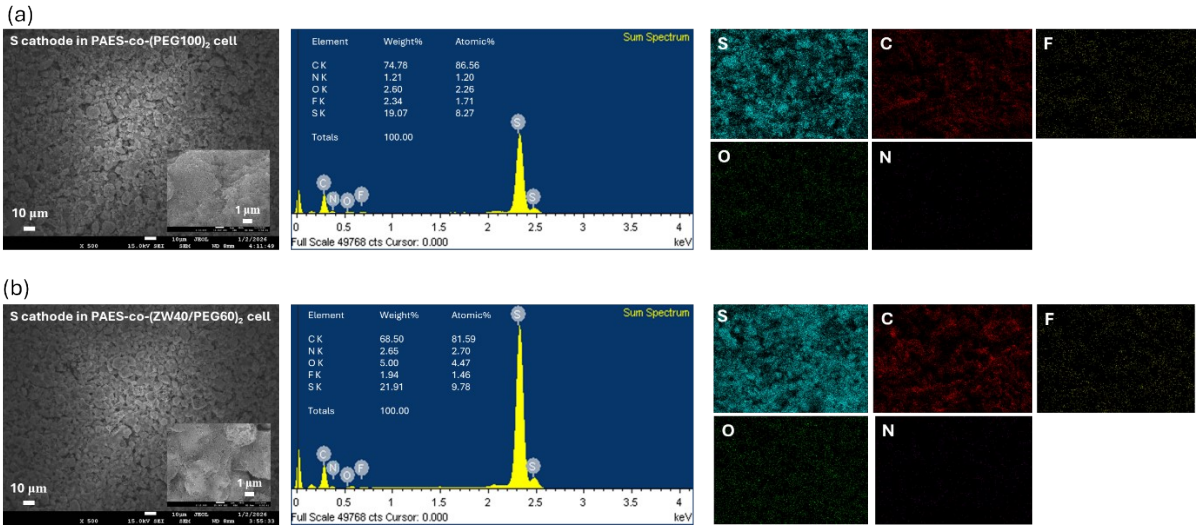

Figure S20. SEM-EDS of cathodic S surface in S/SPE/Li cells assembled with (a) PAES-co-$(PEG100)_2$; and (b) PAES-co-$(ZW40/PEG60)_2$ membranes after cycling at 0.2 C in voltage range of 2.8 -1.5 V.

Table S1. Practical amount of ZW in the prepared PAES-co-(ZW/PEG)$_2$

Electrolyte membrane	Theorical amount of ZW (%)	Intesity of peak		Pratical amount* of ZW (%)
		peak 21 (CH_2 in ZW)	peak 14 (CH_3 in PEG)	
PAES-co-(PEG100)$_2$	0	0	3.987	100
PAES-co-(ZW30/PEG70)$_2$	30	1.587	3.979	28.5
PAES-co-(ZW40/PEG60)$_2$	40	2.322	3.762	38.2
PAES-co-(ZW50/PEG50)$_2$	50	3.124	3.256	49.0
PAES-co-(ZW60/PEG40)$_2$	60	3.896	2.874	57.5
PAES-co-(ZW70/PEG30)$_2$	70	3.902	1.786	68.6

(*) determined by ZW (%) $= \frac{I_{peak\,21}}{I_{peak\,21} + I_{peak\,14}} \times 100$

Table S2. Comparison of ionic conductivity (σ), tensile strength and electrochemical stability window of PAES-co-(ZW40/PEG60)$_2$ membrane with those of other electrolytes recently reported.[1–23]

Electrolyte membranes	σ (mS cm^{-1})	TS [a)] (MPa)	ESW [b)] (V)	[Ref]
Poly(PEG-co-BTA)/zwitterion	4.79	0.05	4.5	[1]
3H-SN-CSSE	1.10	4.87	5.1	[2]
Poly(PEO-co-TFB)/ LiTFSI	0.784	0.137	5.0	[3]
PAES-co-(ZW40/PEG60)$_2$	**1.58**	**1.80**	**5.28**	**Our work**
PL@LCSE 40% *composite*	0.83	0.30	5.0	[4]
D-SPES-PH-PEO	0.741	8.00	5.08	[5]
Poly(MPC-co-SBVI)	0.60	0.116	5.4	[6]
FPH-Li-50	0.418	5.10	4.72	[7]
DPIL-6/ LiTFSI	0.347	0.490	4.9	[8]
PEO/LLZTO *composite*	0.303	0.30	4.8	[9]
PVA-UPy-PEG *co-grafting*	0.287	0.13	5.2	[10]
Sulfide SS-PMSS/ SiO_2 *composite*	0.279	0.15	4.82	[11]
MOF Li-ILs@Co/HPCN	0.191	3.72	5.20	[12]
Cross-linking PBA-co-PMMA/LiTFSI	0.169	15.0	4.8	[13]
PEG-g-UPyMA/ LiPS	0.145	0.50	4.6	[14]
PVT/EMIMTFSI (IL)	0.126	0.04	4.5	[15]
NPE-V_2 *crosslinking electrolyte*	0.0318	1.10	5.10	[16]
Poly(UPy-BCDMA)	0.0293	0.13	5.2	[17]
PEO-LiTFSI-*β*-CD	0.0102	1.60	4.50	[18]
PEG-UPy/ UPy-modified SiO_2 *composite*	0.0088	0.51	5.1	[19]
Poly(HFBM-co-SBMA)/IL	0.0063	0.08	4.7	[20]
PEGDA-UPyMA/ HCP	0.0056	0.40	4.85	[21]
PEG-UPy/ LiTFSI	0.0021	0.274	4.8	[22]
PEG/BPIL	0.0011	2.50	5.0	[23]

[a)] Tensile strength and [b)] electrochemical stability window.

Table S3. Comparison of the S/SEM/Li cell performance based on PAES-co-(ZW40/PEG60)$_2$ membranes with those based on some other electrolytes recently reported. [24–37]

Electrolyte membranes	Discharge capacity (mAh g^{-1})				[Ref]
	0.2C	0.5C	1.0C	2.0C	
PEO/ PIM-8% *gel electrolyte*	1200	1100	910	600	[24]
$Ni_3(HITP)_2$/PP	1186	990	879	790	[25]
NiCoS/PP-P	1050	825	710	520	[26]
PAES-co-(ZW40/PEG60)$_2$	**995.5**	**933.2**	**848.2**	**700.3**	**Our work**
SO_3Li *grafted* UIO (MOF) /LiTFSI +IL	985	890	749	-	[27]
CPE-50wt.%LLTZO *composite*	967	782	673	630	[28]
PEO-$Li_4(BH_4)_3I$/ SiO_2 (5%wt) *composite*	950	817	613	583	[29]
PETT-DA/ (PEO + PVDF-HFP) *nano-fiber*	910	766	624	543	[30]
In-situ S-DCBQ organosulfur	890	795	750	600	[31]
PEO/(LLZO+MWCNT) *composite*	873	810	500	400	[32]
PETEA+divinyladipate/(DOL+TEGDME)	779	621	325	220	[33]
PEO/ (P_2S_5 + LiTFSI) *gel electrolyte*	750	450	-	-	[34]
PEO/ $Li_{1.3}Al_{0.3}Ti_{1.7}(PO_4)_3$/ PEO (*LbL*)	692.9	428.4	362.3	-	[35]
Polydopamine-coated Li_6PS_5Cl *solid*	552.8	226.4	-	-	[36]
PEO/(TCM+ LiTFSI) *solid electrolyte*	450	300	-	-	[37]

Reference

1 K. Deng, S. Zhou, Z. Xu, M. Xiao and Y. Meng, *Chemical Engineering Journal*, 2022, **428**, 131224.

2 W. Zha, J. Li, W. Li, C. Sun and Z. Wen, *Chemical Engineering Journal*, 2021, **406**, 126754.

3 L. Zhang, P. Zhang, C. Chang, W. Guo, Z. H. Guo and X. Pu, *ACS Appl. Mater. Interfaces*, 2021, **13**, 46794–46802.

4 M. Liu, X. Guan, H. Liu, X. Ma, Q. Wu, S. Ge, H. Zhang and J. Xu, *Chemical Engineering Journal*, 2022, **445**, 136436.

5 Q. Yang, M. Liao, P. Ren, D. Li, N. Deng, W. Kang and G. Cai, *Chemical Engineering Journal*, 2024, **495**, 153448.

6 A. J. D'Angelo and M. J. Panzer, *Chem. Mater.*, 2019, **31**, 2913–2922.

7 P. Zhai, Z. Yang, Y. Wei, X. Guo and Y. Gong, *Advanced Energy Materials*, 2022, **12**, 2200967.

8 R. Li, Z. Fang, C. Wang, X. Zhu, X. Fu, J. Fu, W. Yan and Y. Yang, *Chemical Engineering Journal*, 2022, **430**, 132706.

9 H. Zhuang, W. Ma, J. Xie, X. Liu, B. Li, Y. Jiang, S. Huang, Z. Chen and B. Zhao, *Journal of Alloys and Compounds*, 2021, **860**, 157915.

10 Y. H. Jo, B. Zhou, K. Jiang, S. Li, C. Zuo, H. Gan, D. He, X. Zhou and Z. Xue, *Polym. Chem.*, 2019, **10**, 6561–6569.

11 C. Chang, Y. Yao, R. Li, Z. H. Guo, L. Li, C. Pan, W. Hu and X. Pu, *Nano Energy*, 2022, **93**, 106871.

12 Z. Zhang, Y. Huang, H. Gao, C. Li, J. Hang and P. Liu, *Journal of Energy Chemistry*, 2021, **60**, 259–271.

13 B. Zhou, D. He, J. Hu, Y. Ye, H. Peng, X. Zhou, X. Xie and Z. Xue, *J. Mater. Chem. A*, 2018, **6**, 11725–11733.

14 H. Gan, Y. Zhang, S. Li, L. Yu, J. Wang and Z. Xue, *ACS Appl. Energy Mater.*, 2021, **4**, 482–491.

15 X. Tian, P. Yang, Y. Yi, P. Liu, T. Wang, C. Shu, L. Qu, W. Tang, Y. Zhang, M. Li and B. Yang, *Journal of Power Sources*, 2020, **450**, 227629.

16 L. Dong, X. Zeng, J. Fu, L. Chen, J. Zhou, S. Dai and L. Shi, *Chemical Engineering Journal*, 2021, **423**, 130209.

17 B. Zhou, C. Zuo, Z. Xiao, X. Zhou, D. He, X. Xie and Z. Xue, *Chemistry – A European Journal*, 2018, **24**, 19200–19207.

18 H. Duan, L. Li, K. Zou, Y. Deng and G. Chen, *ACS Appl. Mater. Interfaces*, 2021, **13**, 57380–57391.

19 B. Zhou, Y. H. Jo, R. Wang, D. He, X. Zhou, X. Xie and Z. Xue, *J. Mater. Chem. A*, 2019, **7**, 10354–10362.

20 C. Wang, R. Li, P. Chen, Y. Fu, X. Ma, T. Shen, B. Zhou, K. Chen, J. Fu, X. Bao, W. Yan and Y. Yang, *J. Mater. Chem. A*, 2021, **9**, 4758–4769.

21 B. Zhou, M. Yang, C. Zuo, G. Chen, D. He, X. Zhou, C. Liu, X. Xie and Z. Xue, *ACS Macro Lett.*, 2020, **9**, 525–532.

22 L. Chen, X. Cai, Z. Sun, B. Zhang, Y. Bao, Z. Liu, D. Han and L. Niu, *Polymers*, DOI:10.3390/polym13234155.

23 X. Zhu, Z. Fang, Q. Deng, Y. Zhou, X. Fu, L. Wu, W. Yan and Y. Yang, *ACS Sustainable Chem. Eng.*, 2022, **10**, 4173–4185.

24 Y. Ji, K. Yang, M. Liu, S. Chen, X. Liu, B. Yang, Z. Wang, W. Huang, Z. Song, S. Xue, Y. Fu, L. Yang, T. S. Miller and F. Pan, *Advanced Functional Materials*, 2021, **31**, 2104830.

25 Y. Zang, F. Pei, J. Huang, Z. Fu, G. Xu and X. Fang, *Advanced Energy Materials*, 2018, **8**, 1802052.

26 S. Huang, Y. Wang, J. Hu, Y. Von Lim, D. Kong, L. Guo, Z. Kou, Y. Chen and H. Y. Yang, *NPG Asia Materials*, 2019, **11**, 55.

27 P. Chiochan, X. Yu, M. Sawangphruk and A. Manthiram, *Advanced Energy Materials*, 2020, **10**, 2001285.

28 D. Shao, L. Yang, K. Luo, M. Chen, P. Zeng, H. Liu, L. Liu, B. Chang, Z. Luo and X. Wang, *Chemical Engineering Journal*, 2020, **389**, 124300.

29 X. Zhang, T. Zhang, Y. Shao, H. Cao, Z. Liu, S. Wang and X. Zhang, *ACS Sustainable Chem. Eng.*, 2021, **9**, 5396–5404.

30 X. Wang, X. Hao, Z. Hengjing, X. Xia and J. Tu, *Electrochimica Acta*, 2020, **329**, 135108.

31 K. Chen, R. Fang, Z. Lian, X. Zhang, P. Tang, B. Li, K. He, D. Wang, H.-M. Cheng, Z. Sun and F. Li, *Energy Storage Materials*, 2021, **37**, 224–232.

32 R.-A. Tong, L. Chen, G. Shao, H. Wang and C.-A. Wang, *Journal of Power Sources*, 2021, **492**, 229672.

33 H. Du, S. Li, H. Qu, B. Lu, X. Wang, J. Chai, H. Zhang, J. Ma, Z. Zhang and G. Cui, *Journal of Membrane Science*, 2018, **550**, 399–406.

34 S. Chen, B. Ding, Q. Lin, Y. Shi, B. Hu, Z. Li, H. Dou and X. Zhang, *Journal of Electroanalytical Chemistry*, 2021, **880**, 114874.

35 A. Santiago, J. Castillo, I. Garbayo, A. Saenz de Buruaga, J. A. Coca Clemente, L. Qiao, R. Cid Barreno, M. Martinez-Ibañez, M. Armand, H. Zhang and C. Li, *ACS Appl. Energy Mater.*, 2021, **4**, 4459–4464.

36 Y. Wang, G. Wang, P. He, J. Hu, J. Jiang and L.-Z. Fan, *Chemical Engineering Journal*, 2020, **393**, 124705.

37 G. Liu, J. Shi, M. Zhu, W. Weng, L. Shen, J. Yang and X. Yao, *Energy Storage Materials*, 2021, **38**, 249–254.